How to cite: *Angew. Chem. Int. Ed.* **2021**, *60*, 4018–4022
International Edition: doi.org/10.1002/anie.202013069
German Edition: doi.org/10.1002/ange.202013069

Polymerization Catalysis

Efficient Suppression of Chain Transfer and Branching via C_s-Type Shielding in a Neutral Nickel(II) Catalyst

Chaoqun Wang[+], Xiaohui Kang[+], Shengyu Dai[+], Fengchao Cui, Yunqi Li, Hongliang Mu, Stefan Mecking, and Zhongbao Jian**

Abstract: *An effective shielding of both apical positions of a neutral Ni^{II} active site is achieved by dibenzosuberyl groups, both attached via the same donors' N-aryl group in a C_s-type arrangement. The key aniline building block is accessible in a single step from commercially available dibenzosuberol. This shielding approach suppresses chain transfer and branch formation to such an extent that ultrahigh molecular weight polyethylenes (5×10^6 g mol^{-1}) are accessible, with a strictly linear microstructure (< 0.1 branches/1000C). Key features of this highly active (4.3×10^5 turnovers h^{-1}) catalyst are an exceptionally facile preparation, thermal robustness (up to 90 °C polymerization temperature), ability for living polymerization and compatibility with THF as a polar reaction medium.*

Compared to traditional olefin polymerization catalysts based on d^0-metal sites,[1,2] late transition metal catalysts offer benefits such as a tolerance towards polar substrates and reaction media.[3–6] Late transition metal complexes are generally prone to β-hydride elimination (BHE), however. This results in chain transfer and branch formation pathways. To achieve substantial polymer molecular weights, an effective suppression of these pathways that compete with chain growth is essential. Accessing ultrahigh molecular weight polyethylenes[7,8] (UHMWPEs) requires a 10^5-fold favoring of chain growth events over chain transfers.

In olefin polymerization with late transition metal Ni^{II} and Pd^{II} catalysts, high polymer molecular weights are favored by steric shielding of apical positions which hinders chain transfer by associative displacement.[9–15] The most efficient way of doing so is arrangement of aryl groups parallel to the square-planar coordination plane, above and below the active site. Several examples for κ^2-N,N diimine complexes are based on the principle of a C_2-type arrangement of the shielding groups, by attaching each shielding group via the substituent framework of one donor.

To transfer this approach to neutral complexes with their unsymmetric κ^2-X,Y-chelating environment, both different donors' substitution pattern needs to be suited for attachment of a shielding "lid". Brookhart and Daugulis solved this elegantly by using enolatoimine complexes most recently (Scheme 1; bottom, left).[16] This approach is not generally applicable to other popular neutral catalyst motifs, however, in which the hard oxygen donor is surrounded by a ligand framework less suitable to achieve C_2-type shielding. Thus, for the popular and versatile salicylaldiminato motif[17–20] so far only a parallel shielding on one side has been achieved, by means of *N*-(8-phenylnaphty-1-yl) groups (Scheme 1; bottom, right).[21,22]

We now show how an effective shielding on both apical positions can be achieved by a C_s-type arrangement. This is achieved via readily accessible dibenzosuberyl substituents, and affords strictly linear UHMWPE devoid of any branches.

Catalyst Design

As a reference point, a set of dibenzhydryl[23,24] (Ar_2CH-) substituted salicylaldimines covering a range of steric and electronic properties were generated, and converted to corresponding Ni^{II} complexes (**Ni2** to **Ni10**, Scheme 2; for

[*] C. Wang,[+] Prof. Dr. Y. Li, Dr. H. Mu, Prof. Dr. Z. Jian
State Key Laboratory of Polymer Physics and Chemistry, Changchun Institute of Applied Chemistry, Chinese Academy of Sciences
Renmin Street 5625, Changchun 130022 (China)
E-mail: zbjian@ciac.ac.cn
C. Wang,[+] Prof. Dr. Z. Jian
University of Science and Technology of China
Hefei 230026 (China)
Prof. Dr. S. Mecking
Chair of Chemical Materials Science, Department of Chemistry, University of Konstanz
78457 Konstanz (Germany)
E-mail: stefan.mecking@uni-konstanz.de
Prof. Dr. X. Kang[+]
College of Pharmacy, Dalian Medical University
Dalian 116044 (China)
Prof. Dr. S. Dai[+]
Institutes of Physical Science and Information Technology, Key Laboratory of Structure and Functional Regulation of Hybrid Materials of Ministry of Education, Anhui University
Hefei, Anhui, 230601 (China)
Prof. Dr. F. Cui
Key laboratory of Polyoxometalate Science of the Ministry of Education, Faculty of Chemistry, Northeast Normal University
Changchun 130024 (China)
[+] These authors contributed equally to this work.
Supporting information and the ORCID identification number(s) for the author(s) of this article can be found under: https://doi.org/10.1002/anie.202013069.

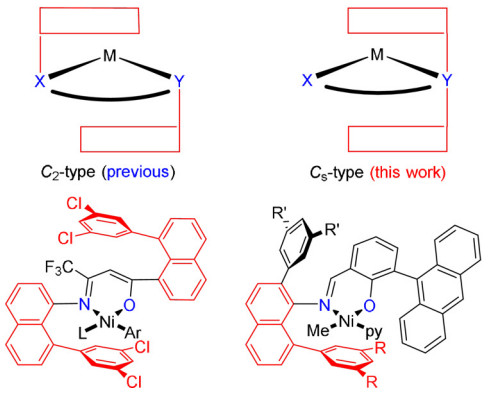

Scheme 1. C_2-type arrangement of aryl substituents parallel to the coordination plane (top, left) and C_s-approach pursued in this work (top, right). C_2-type shielded neutral enolatoimine Ni^{II} complex (bottom, left). C_1-type *N*-(8-phenylnaphty-1-yl) salicylaldiminato Ni^{II} complex (bottom, right).

full synthesis and characterization of metal complexes and ligands cf. the Supporting Information, SI). Additionally, the prototypical reference **Ni1** was prepared by a reported procedure (Scheme 2).[17]

Without addition of any activating cocatalysts, these neutral single-component Ni^{II} catalysts were evaluated for ethylene polymerization under 8 bar at various temperatures. Despite

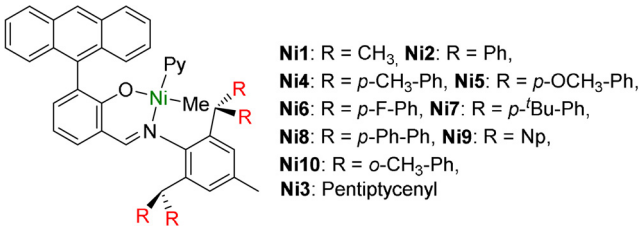

Ni1: R = CH_3, **Ni2**: R = Ph,
Ni4: R = *p*-CH_3-Ph, **Ni5**: R = *p*-OCH_3-Ph,
Ni6: R = *p*-F-Ph, **Ni7**: R = *p*-^{t}Bu-Ph,
Ni8: R = *p*-Ph-Ph, **Ni9**: R = Np,
Ni10: R = *o*-CH_3-Ph,
Ni3: Pentiptycenyl

Scheme 2. Reference Ni^{II} catalysts studied.

their considerably different steric and electronic substitution patterns, **Ni1**–**Ni10** did not differ dramatically in their catalytic properties (Table 1 and Figure 1; cf. SI for full polymerization data).

To rationalize these findings, steric maps based on single crystal structures were optimized by a DFT method (BP86-D3 method, cf. SI for computational details) and the buried volume (V_{bur}) as a measure of the steric environment around the active Ni^{II} site was calculated[25] (Figure 2). Notably, despite their sterically demanding substituents **Ni8** (*p*-Ph-Ph) and **Ni9** (Np) feature a similar—even slightly lower—V_{bur}% value than **Ni2** (Ph) (45% and 46% vs. 48%).

Viewing the substituents in single crystal maps, we find that due to their free rotation, these bulky substituents such as Ph, *p*-Ph-Ph, and Np consistently orient away from the Ni^{II} active center (cf. SI. Notably, solution NMR data of **Ni2** confirms

Table 1: Ethylene polymerization with reference Ni^{II} catalysts.[a]

Entry	cat.	*T* [°C]	Yield [g]	act. [×10^6][b]	M_n [×10^4][c]	M_w [×10^4][c]	M_w/M_n[c]	brs[d]	T_m[e] [°C]
1	**Ni1**	30	0.72	0.58	11.8	16.5	1.40	3	129
2	**Ni1**	90	0.56	0.45	0.6	0.8	1.44	63	/
3	**Ni2**	30	1.94	1.55	27.3	31.9	1.17	3	134
4	**Ni2**	90	1.33	1.06	0.6	1.1	1.77	61	81
5	**Ni3**	30	0.61	0.49	8.5	12.6	1.47	3	135
6	**Ni3**	90	3.31	2.65	0.4	0.4	1.15	43	101
7	**Ni4**	30	0.88	0.70	14.6	19.0	1.30	3	134
8	**Ni4**	90	2.18	1.74	0.7	1.2	1.55	65	80
9	**Ni5**	30	0.63	0.50	15.0	18.2	1.21	2	135
10	**Ni5**	90	2.53	2.02	0.9	1.2	1.35	63	79
11	**Ni6**	30	0.84	0.67	17.8	22.0	1.24	3	136
12	**Ni6**	90	2.32	1.86	0.6	0.9	1.46	60	85
13	**Ni7**	30	1.60	1.28	25.6	30.4	1.19	2	133
14	**Ni7**	90	2.29	1.83	0.7	1.3	1.95	62	78
15	**Ni8**	30	0.83	0.66	14.3	17.7	1.24	10	133
16	**Ni8**	90	2.53	2.02	0.7	1.4	1.92	53	85
17	**Ni9**	30	0.94	0.75	14.0	18.7	1.34	6	129
18	**Ni9**	90	1.22	0.98	0.3	0.5	1.48	84	/
19	**Ni10**	30	2.31	1.85	22.5	31.4	1.40	11	118
20	**Ni10**	90	0.80	0.64	1.1	1.8	1.70	55	/
21	**Ni11**	30	2.93	2.34	57.4	67.2	1.17	3	132
22	**Ni11**	50	3.94	3.15	39.9	70.4	1.77	14	123
23	**Ni11**	70	1.87	1.50	32.4	53.1	1.64	23	106
24	**Ni11**	90	1.65	1.32	9.5	16.9	1.78	46	84
25	**Ni12**	30	2.00	1.60	63.7	73.9	1.16	4	128
26	**Ni12**	50	1.75	1.40	44.2	71.9	1.63	17	110
27	**Ni12**	70	0.95	0.76	18.5	32.8	1.77	42	83
28	**Ni12**	90	0.78	0.62	10.0	17.6	1.76	74	/
29[f]	**Ni11**	50	4.61	3.69	36.1	56.0	1.55	14	118

[a] Reaction conditions: Ni catalyst (5 µmol), toluene (100 mL), ethylene (8 bar), polymerization time (15 min), all entries are based on at least two runs, unless noted otherwise. [b] Activity is in unit of 10^6 g mol^{-1} h^{-1}. [c] Determined by GPC in 1,2,4-trichlorobenzene at 150 °C using a light scattering detector. [d] brs = Number of branches per 1000C, as determined by ^{1}H NMR spectroscopy. [e] Determined by DSC (second heating). [f] THF (100 mL) as solvent.

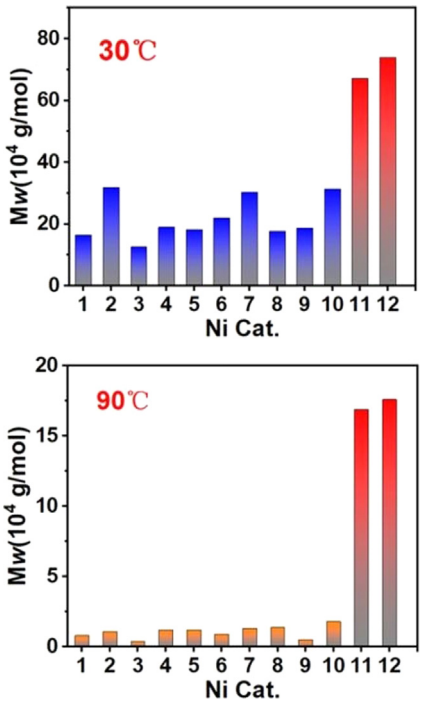

Figure 1. Polymer molecular weights produced by **Ni1**–**Ni12** at 30 °C and 90 °C, respectively (8 bar ethylene).

free rotation of the phenyl groups around the CH-Ph bond, cf. SI). As a consequence, shielding of the axial sites to retard β-H elimination is limited. Most notably, the axial sites above and below the square planar coordinated Ni^{II} center are not both shielded (Figure 2 a–d).

To appropriately restrict conformational freedom and force an aryl ring into each apical position, we sought to annulate a given dibenzhydryl moieties' aryl groups to a suitable mutual ring structure. In view of its considerable tension, a seven-membered ring in the form of a dibenzosuberyl motif[26] was targeted.

Remarkably, the key 2,6-disubstituted aniline is accessible in a single step from commercially available compounds in good yield (70 %, Scheme 3). This contrasts the multi-step synthesis of the aniline component for state-of-the-art *N*-terphenyl- and *N*-8-arylnaphthyl- salicylaldiminato Ni^{II} catalysts[21,22,27,28] (cf. Scheme 1).

Condensation with salicylaldehydes, and reaction with [(tmeda)$NiMe_2$] and pyridine yielded dibenzosuberyl-based 9-anthracenyl- and *meta*-terphenyl-substituted salicylaldiminato Ni^{II} complexes **Ni11** and **Ni12**, respectively (Scheme 3. For full characterization data cf. the SI). **Ni11** and **Ni12** were undoubtedly corroborated by NMR spectroscopy and elemental analysis. Based on single crystal structure data (cf. SI for details), the buried volume of **Ni11** was determined by the aforementioned DFT methods. This yields a significantly higher value compared to the reference cases (V_{bur}% value 52 %). Most significantly, two dibenzosuberyl substituents very effectively shield the axial sites above and below the square planar Ni^{II} center (Figure 2 e). This effective shielding by the suberyl aryl groups is also reflected by an upfield ^{1}H NMR resonance of the Ni-Me moiety (**Ni11**: −0.93 ppm) relative to the reference catalyst precursors (**Ni2**: −0.29 ppm). Most notably, in pressure reactor ethylene polymerization experiments with **Ni11** and **Ni12** yield much higher molecular weights vs. all reference systems (Table 1 and Figure 1).

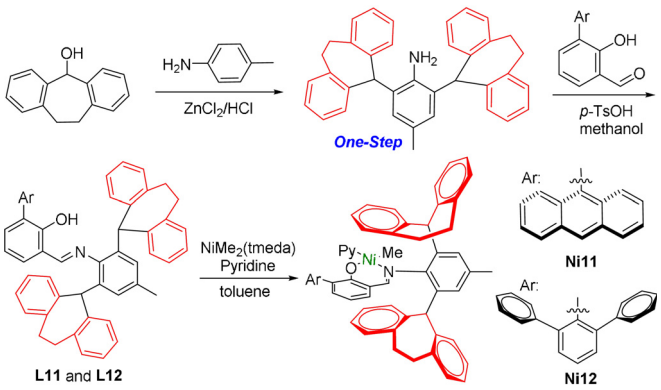

Scheme 3. Synthesis of C_s-shielded neutral salicylaldiminato Ni^{II} catalysts.

Polymerization properties

Ethylene polymerization with **Ni11** and **Ni12** as single-component catalyst precursors was studied in more detail (Table 1, entries 21–28 and Table 2). Notably, **Ni11** and **Ni12** are thermally robust to give a high molecular weight (M_w = 16.9×10^4 g mol^{-1}) even at a high polymerization temperature of 90 °C, more than an order of magnitude higher than those produced by **Ni1**–**Ni10** (Figure 1), indicating the effectiveness of our C_s-type shielding strategy.

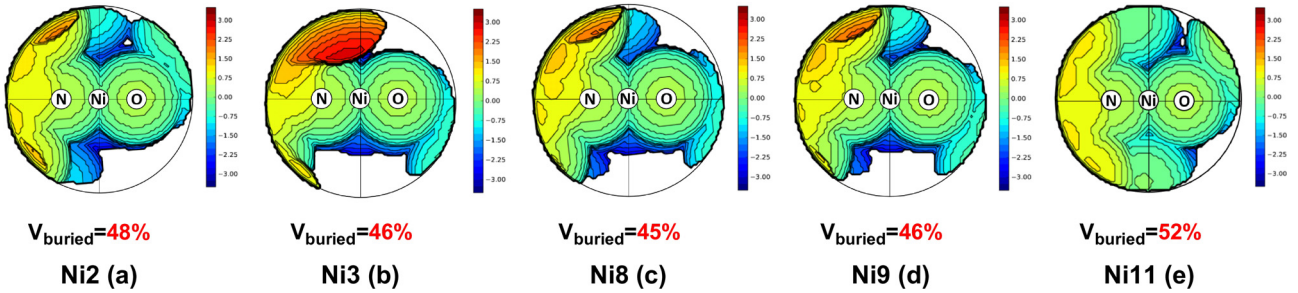

Figure 2. Steric maps of **Ni2**, **Ni3**, **Ni8**, **Ni9**, and **Ni11** optimized by a DFT computational method (BP86-D3).

Table 2: Effect of time and pressure on ethylene polymerization with **Ni11**.[a]

Entry	T [°C]	P [bar]	T [min]	Yield [g]	act. [$\times 10^6$][b]	M_n [$\times 10^4$][c]	M_w [$\times 10^4$][c]	M_w/M_n[c]	brs[d]	T_m[e] [°C]
1[f]	30	8	5	0.31	2.19	22.3	25.5	1.15	3.5	131/135
2[f]	30	8	10	0.60	2.12	39.5	45.4	1.15	2.9	133/136
3[f]	30	8	15	0.91	2.14	57.8	69.5	1.20	2.7	133/138
4[f]	30	8	20	1.09	1.92	70.9	86.5	1.22	2.9	132/ 138
5[g]	30	30	15	2.61	6.96	208.7	242.3	1.16	0.2[k]	136/ 144
6[h]	30	40	15	2.26	12.05	248.9	372.2	1.50	0.1[k]	134/142
7[h]	30	40	60	2.95	3.93	304.7	505.1	1.66	<0.1[k]	135/144
8[i]	90	30	15	2.94	3.92	21.1	31.8	1.51	29	99/106
9[i]	90	40	15	3.70	4.93	22.4	34.1	1.52	28	101/106
10[h,j]	30	40	60	2.31	3.08	141.3	202.0	1.43	0.3[k]	135/143

[a] Reaction conditions: toluene (100 mL), all entries are based on at least two runs, unless noted otherwise. [b] Activity is in unit of 10^6 g mol^{-1} h^{-1}. [c] Determined by GPC in 1,2,4-trichlorobenzene at 150 °C using a light scattering detector. [d] brs = Number of branches per 1000C, as determined by ^{1}H NMR spectroscopy. [e] Determined by DSC at 10 K min^{-1} (second heating/ first heating). [f] **Ni11** (1.7 μmol). [g] **Ni11** (1.5 μmol). [h] **Ni11** (0.75 μmol). [i] **Ni11** (3 μmol). [j] THF (100 mL). [k] brs = Number of branches per 1000C, as determined by ^{13}C NMR spectroscopy.

Compared to these polymerizations in toluene, catalytic activity is even higher in tetrahydrofuran (THF) as a polar reaction medium, although molecular weight decreases slightly (Table 1, entries 22 vs. 29). Remarkably, polymerization even occurs in this challenging reaction medium—which is not compatible with early transition metal and also many late metal polymerization catalysts[3–6,20]—to high molecular weight polymer (Table 2).

The polymerization to high molecular weight polyethylenes proceeds in a living fashion at 30 °C and 8 bar (Table 2, entries 1–4). Both yield and molecular weight increase linearly with polymerization time (Figure 3). Within 20 min $M_w = 86.5 \times 10^4$ g mol^{-1} is reached. Notably, polymer precipitation during the reaction possibly has a small effect on molecular weight distributions.

Polymerization at higher 40 bar ethylene pressure results in remarkably higher catalyst activities (TOF: 4.3×10^5 h^{-1}) and molecular weights well in the ultrahigh molecular weight regime (M_w: 3.7×10^6 g mol^{-1}), while branching is further reduced to only 0.1/1000C (Table 2, entry 6). This compares favorably with the state-of-the-art neutral Ni^{II} catalysts[16,21,28] and other catalysts.[29–32]

Due to the triple characteristics of high activity, low degree of branching, and ultrahigh molecular weight, rapid precipitation of the product polymer occurred during polymerization, which may impact the reaction. Thus, an even lower catalyst loading of 7.5×10^{-7} mol was explored. Notably, despite the absence of any alkyl aluminum cocatalysts or scavenger, polymerization performance is retained (Table 2, entries 6 and 7). At a prolonged reaction time of 1 h UHWMPE with M_w of 5.1×10^6 g mol^{-1} (M_n: 3.1×10^6 g mol^{-1}) is formed. Most importantly, the degree of branching is below the detection limit (<0.1/1000C) (Figure 4, Table 2, entry 7). This is also reflected in a very high melting point (T_m) of up to 144 °C. As anticipated, higher ethylene pressure of 30 bar and 40 bar at challenging 90 °C resulted in elevated activities and enhanced molecular weights (M_w: 3.4×10^5 g mol^{-1}) (Table 2, entries 8 and 9). Most notably, in THF as a reaction medium **Ni11** even enabled the formation of linear UHMWPE (M_w: 2.0×10^6 g mol^{-1}; 0.3 branches/1000C) at 40 bar (Table 2, entry 10). **Ni11** was also capable of promoting copolymerization of ethylene and ester-functionalized undecylenic acid methyl ester (cf. SI, Table S2). Studies at various temperatures from 30 °C to 90 °C gave copolymers with high molecular weights (3.9 to 26.4×10^4 g mol^{-1}), tunable degrees of branching (4 to 28/1000C), and reasonable incorporations of comonomer (0.2 to 1.5 mol %).

In summary, the approach reported enables an effective shielding of both apical positions of a square-planar coordinated active metal site, through a C_s-type arrangement of both shielding groups by attachment via the same N-donor

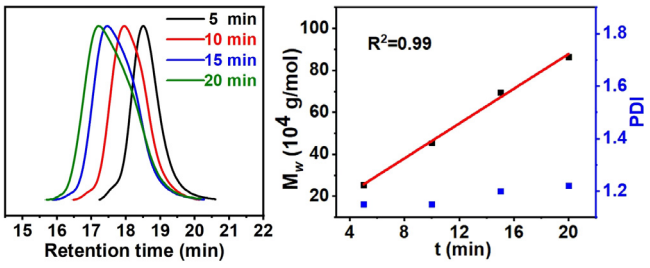

Figure 3. Living nature of ethylene polymerization with **Ni11** at 30 °C (Table 2, entries 1–4).

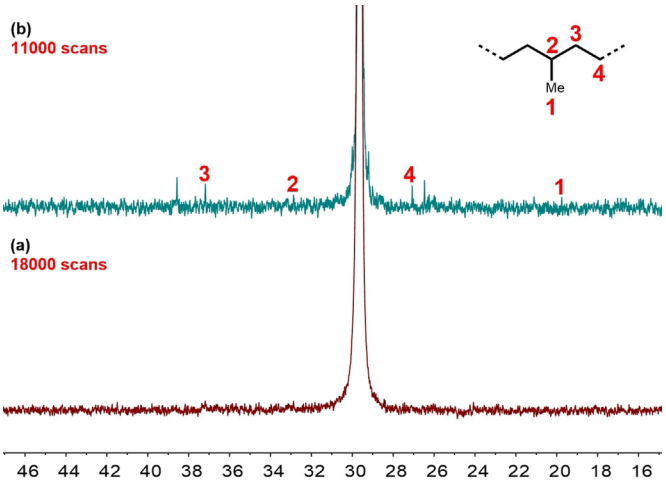

Figure 4. ^{13}C NMR spectra (100 MHz, $C_2D_2Cl_4$, 110 °C) of strictly linear UHMWPEs (conc.: 100 g L^{-1}): a) Table 2, entry 7; b) Table 2, entry 5.

atoms' framework. This overcomes the general propensity of late transition metal catalysts for β-H elimination, and hinders chain transfer and branching pathways very effectively, as evidenced by a living nature of the polymerization and the formation of strictly linear ultrahigh molecular weight polyethylene. Such a microstructure is desirable for this important material, but difficult to access, particularly with late transition metal catalysts. Notably, these novel catalysts are also thermally robust and tolerant to polar reaction media. At the same time, this novel type of shielding is easily accessible. The key aniline building block is formed from commercially available compounds in a single step, with good yield. Thus, this chemistry provides broader perspectives for polymerization catalysis and beyond.

Acknowledgements

Z.J. and X.K. are thankful for financial support from the National Natural Science Foundation of China (Nos. 21871250 and 21704011), the Jilin Provincial Science and Technology Department Program (No. 20200801009GH). Open access funding enabled and organized by Projekt DEAL.

Conflict of interest

The authors declare no conflict of interest.

Keywords: coordination polymerization · C_s shielding · homogeneous catalysis · linear UHMWPE · nickel catalyst

[1] M. Stürzel, S. Mihan, R. Mülhaupt, *Chem. Rev.* **2016**, *116*, 1398 – 1433.
[2] M. C. Baier, M. A. Zuideveld, S. Mecking, *Angew. Chem. Int. Ed.* **2014**, *53*, 9722 – 9744; *Angew. Chem.* **2014**, *126*, 9878 – 9902.
[3] Z. Chen, M. Brookhart, *Acc. Chem. Res.* **2018**, *51*, 1831 – 1839.
[4] A. Nakamura, S. Ito, K. Nozaki, *Chem. Rev.* **2009**, *109*, 5215 – 5244.
[5] A. Keyes, H. E. Basbug Alhan, E. Ordonez, U. Ha, D. B. Beezer, H. Dau, Y. S. Liu, E. Tsogtgerel, G. R. Jones, E. Harth, *Angew. Chem. Int. Ed.* **2019**, *58*, 12370 – 12391; *Angew. Chem.* **2019**, *131*, 12498 – 12520.
[6] C. Tan, C. Chen, *Angew. Chem. Int. Ed.* **2019**, *58*, 7192 – 7200; *Angew. Chem.* **2019**, *131*, 7268 – 7276.
[7] S. M. Kurtz, *A Primer on UHMWPE. UHMWPE biomaterials handbook*, 3rd ed. (Ed.: S. M. Kurtz), William Andrew Publishing, Oxford, **2016**.
[8] K. Patel, S. H. Chikkali, S. Sivaram, *Prog. Polym. Sci.* **2020**, *109*, 101290.
[9] L. K. Johnson, C. M. Killian, M. Brookhart, *J. Am. Chem. Soc.* **1995**, *117*, 6414 – 6415.
[10] D. H. Camacho, E. V. Salo, J. W. Ziller, Z. Guan, *Angew. Chem. Int. Ed.* **2004**, *43*, 1821 – 1825; *Angew. Chem.* **2004**, *116*, 1857 – 1861.
[11] D. Zhang, E. T. Nades, M. Brookhart, O. Daugulis, *Organometallics* **2013**, *32*, 5136 – 5143.
[12] T. Vaidya, K. Klimovica, A. M. LaPointe, I. Keresztes, E. B. Lobkovsky, O. Daugulis, G. W. Coates, *J. Am. Chem. Soc.* **2014**, *136*, 7213 – 7216.
[13] K. E. Allen, J. Campos, O. Daugulis, M. Brookhart, *ACS Catal.* **2015**, *5*, 456 – 464.
[14] K. S. O'Connor, A. Watts, T. Vaidya, A. M. LaPointe, M. A. Hillmyer, G. W. Coates, *Macromolecules* **2016**, *49*, 6743 – 6751.
[15] K. S. O'Connor, J. R. Lamb, T. Vaidya, I. Keresztes, K. Klimovica, A. M. LaPointe, O. Daugulis, G. W. Coates, *Macromolecules* **2017**, *50*, 7010 – 7027.
[16] Q. H. Tran, M. Brookhart, O. Daugulis, *J. Am. Chem. Soc.* **2020**, *142*, 7198 – 7206.
[17] T. R. Younkin, E. F. Connor, J. I. Henderson, S. K. Friedrich, R. H. Grubbs, D. A. Bansleben, *Science* **2000**, *287*, 460 – 462.
[18] D. Takeuchi, Y. Chiba, S. Takano, K. Osakada, *Angew. Chem. Int. Ed.* **2013**, *52*, 12536 – 12540; *Angew. Chem.* **2013**, *125*, 12768 – 12772.
[19] M. R. Radlauer, A. K. Buckley, L. M. Henling, T. Agapie, *J. Am. Chem. Soc.* **2013**, *135*, 3784 – 3787.
[20] H. Mu, L. Pan, D. Song, Y. Li, *Chem. Rev.* **2015**, *115*, 12091 – 12137.
[21] Z. Chen, M. Mesgar, P. S. White, O. Daugulis, M. Brookhart, *ACS Catal.* **2015**, *5*, 631 – 636.
[22] P. Kenyon, M. Wörner, S. Mecking, *J. Am. Chem. Soc.* **2018**, *140*, 6685 – 6689.
[23] X. Hu, S. Dai, C. Chen, *Dalton Trans.* **2016**, *45*, 1496 – 1503.
[24] J. L. Rhinehart, L. A. Brown, B. K. Long, *J. Am. Chem. Soc.* **2013**, *135*, 16316 – 16319.
[25] L. Falivene, Z. Cao, A. Petta, L. Serra, A. Poater, R. Oliva, V. Scarano, L. Cavallo, *Nat. Chem.* **2019**, *11*, 872 – 879.
[26] Q. Mahmood, Y. Zeng, E. Yue, G. A. Solan, T. Liang, W.-H. Sun, *Polym. Chem.* **2017**, *8*, 6416 – 6430.
[27] M. Schnitte, J. S. Scholliers, K. Riedmiller, S. Mecking, *Angew. Chem. Int. Ed.* **2020**, *59*, 3258 – 3263; *Angew. Chem.* **2020**, *132*, 3284 – 3289.
[28] M. Schnitte, A. Staiger, L. A. Casper, S. Mecking, *Nat. Commun.* **2019**, *10*, 2592.
[29] A. L. Kocen, M. Brookhart, O. Daugulis, *Nat. Commun.* **2019**, *10*, 438.
[30] L. Guo, S. Dai, C. Chen, *Polymers* **2016**, *8*, 37.
[31] S. Dai, C. Chen, *Angew. Chem. Int. Ed.* **2016**, *55*, 13281 – 13285; *Angew. Chem.* **2016**, *128*, 13475 – 13479.
[32] T. Liang, S. B. Goudari, C. Chen, *Nat. Commun.* **2020**, *11*, 372.

Manuscript received: September 27, 2020
Accepted manuscript online: November 17, 2020
Version of record online: December 23, 2020

